

0895-3996/95 \$12.00

Copyright © 1995 by Academic Press, Inc.
All rights of reproduction in any form reserved.

Bragg X-Ray Optics for Imaging Spectroscopy of Plasma Microsources¹

T. A. PIKUZ,* A. YA. FAENOV,* S. A. PIKUZ,[†]
V. M. ROMANOVA,[†] AND T. A. SHELKOVENKO[†]

*NPO VNIIFTRI, Mendeleev, Moscow Region, Russia; and [†]P. N. Lebedev Physics Institute,
Russian Academy of Sciences, Moscow, Russia

Received October 26, 1994; revised May 10, 1995

Bragg x-ray optics based on crystals with transmission and reflection properties bent on cylindrical or spherical surfaces are discussed. Applications of such optics for obtaining one- and two-dimensional monochromatic images of different plasma sources in the wide spectral range 1–20 Å are described. Samples of spectra obtained with spectral resolution of up to $\lambda/\Delta\lambda \sim 10,000$ and spatial resolution of up to 18 μm are presented. © 1995 Academic Press, Inc.

INTRODUCTION

X-ray emission of multicharged ions in the spectral range from 1 to 20 Å produces the most fundamental information about the parameters of hot and dense plasmas. This fact plus the diversity of practical x-ray applications motivated numerous investigations in this field. At the present time the spectral range from 4 to 20 Å, which includes the emission spectra of many multicharged ions of the light elements, has been studied fairly well. However, presently only a small number of x-ray spectroscopic devices achieve sufficiently high spectral resolution in this range.

An even more difficult situation exists for the registration of x-ray emission lines with wavelengths from 1 to 3 Å. This spectral range is dominated by the radiation of multicharged ions of heavy elements. The relatively low intensity and very complicated spectral structure of such emissions require the employment of special devices with high luminosity and high resolution. The maximum spectral resolution will be achieved when the Bragg angles are close to the normal incidence of the beam. Due to this condition, short-wavelength x-ray spectrographs must be composed of crystals with very small interplanar spacings approximately equal to the wavelengths of the radiation being investigated. Due to the reasons mentioned above, improvements in spectral and space resolution and luminosity of the spectral devices are necessary.

The elements of the high-performance x-ray optics that are used for investigations

¹ This paper was presented at the International Conference on Short Wavelength Radiation and Applications held in Zvenigorod, Russia, August 29–September 2, 1994.

of x-ray radiation of different plasma microsources are shown in Fig. 1. The elements of x-ray optics can be divided into two main groups according to their application, either obtaining highly resolved spectra or obtaining plasma images with one- or two-dimensional spatial resolution. In this report we describe only the most interesting, which in our opinion are the focusing spectrographs. These include (1) spectrographs with spherically bent crystals for obtaining spectral images of the plasma sources with one- or two-dimensional spatial resolution, FSSR-1D and FSSR-2D (*Focusing Spectrograph with Spatial Resolution*), and (2) Cauchois-type spectrographs with slits placed parallel to the direction of dispersion. We will also briefly discuss below some results of the development and testing of such Bragg crystal spectrographs. In this case we emphasize the unique role of the laser-produced plasmas and the plasmas of Z- and X-pinch devices for precise testing of the x-ray optics. This is mostly due to the very small sizes of such sources (up to 5–10 μm) and high brightness in all spectral ranges from 1 to 26 Å, where most crystals operate.

SPECTRAL DEVICES WITH SPHERICALLY BENT CRYSTALS

Focusing spectrographs with one-dimensional spatial resolution (FSSR-1D). The use of crystals bent along a cylindrical surface instead of flat crystals has made it possible to increase the luminosity of an x-ray spectrograph by one to two orders of magnitude. Further increases of luminosity require using crystals bent on surfaces of double curvature, which can be toroidal, elliptical, spherical, etc. In the case of a crystal bent on a spherical surface, the focusing of the spectrum occurs in the same way as a crystal bent along a cylindrical surface, i.e., on the Rowland circle (see Fig. 2). The main difference is that in a spherically bent crystal there is also focusing at right angles to the direction of the dispersion. The focal length of a spherical mirror in this direction, i.e., in the saggital plane, is determined by the geometric optics condition $f = R/2 \sin \theta$, where R is the radius of the surface of the crystal and θ is the grazing angle determined by the Bragg equation $2d \sin \theta = m\lambda$, where m is the order of reflection from crystal and d is the interplanar spacing of the crystal. Thus, the condition for focusing at right angles to the direction of dispersion varies with the wavelength of the radiation being recorded. The magnification in the case of full focusing in both meridional (spectral focusing) and saggital (space focusing) planes is given by

$$K = b/a = \cos 2\varphi = 2(m\lambda/2d)^2 - 1, \quad [1]$$

where $a = R \cos \varphi/\cos 2\varphi$ and $b = R \cos \varphi$ are the distances from the source to the crystal and from the crystal to the photographic film respectively; φ is the angle of the radiation incident to the crystal. This scheme obtains highly resolved spectra with very good one-dimensional spatial resolution. The main problem with using this scheme is the large radius of curvature for the small crystals used previously, such as quartz and KAP. These crystals obtained spectra only in a very narrow spectral range in the vicinity of one spectral line. The technology for bending large mica crystals on very small radii made it possible to use the FSSR schemes successfully

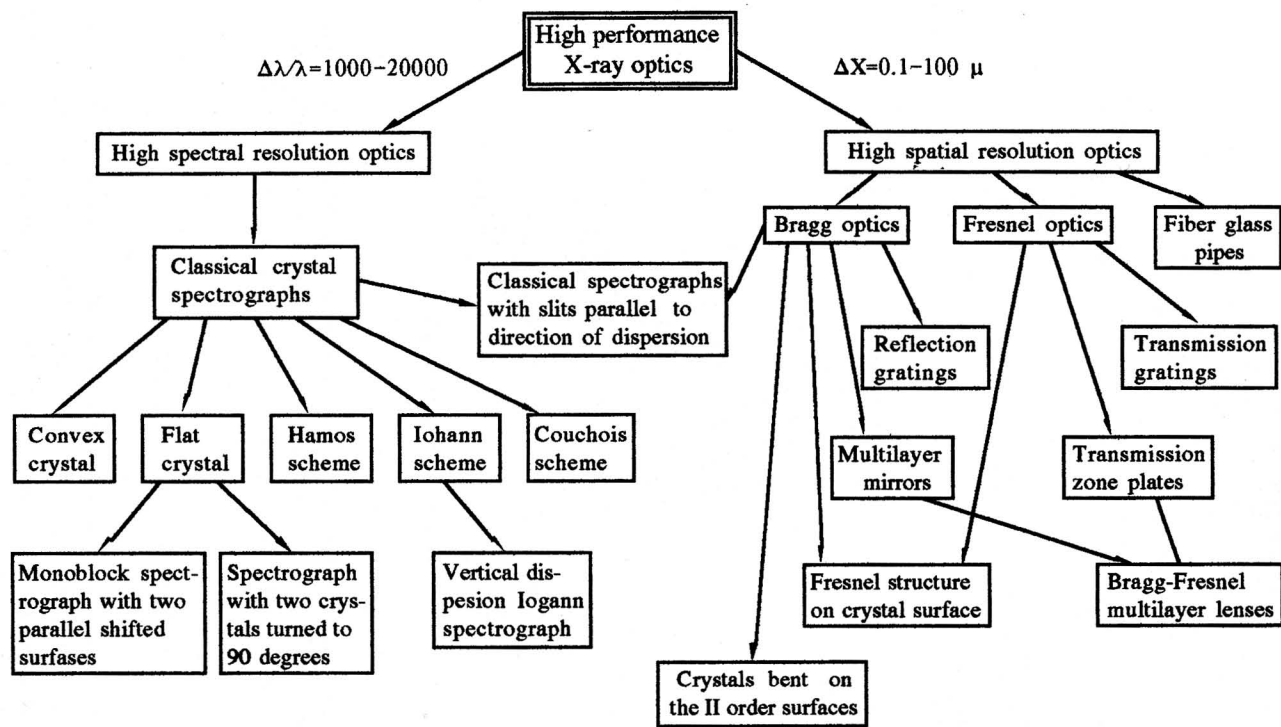


FIG. 1. Types and applications of different spectral devices.

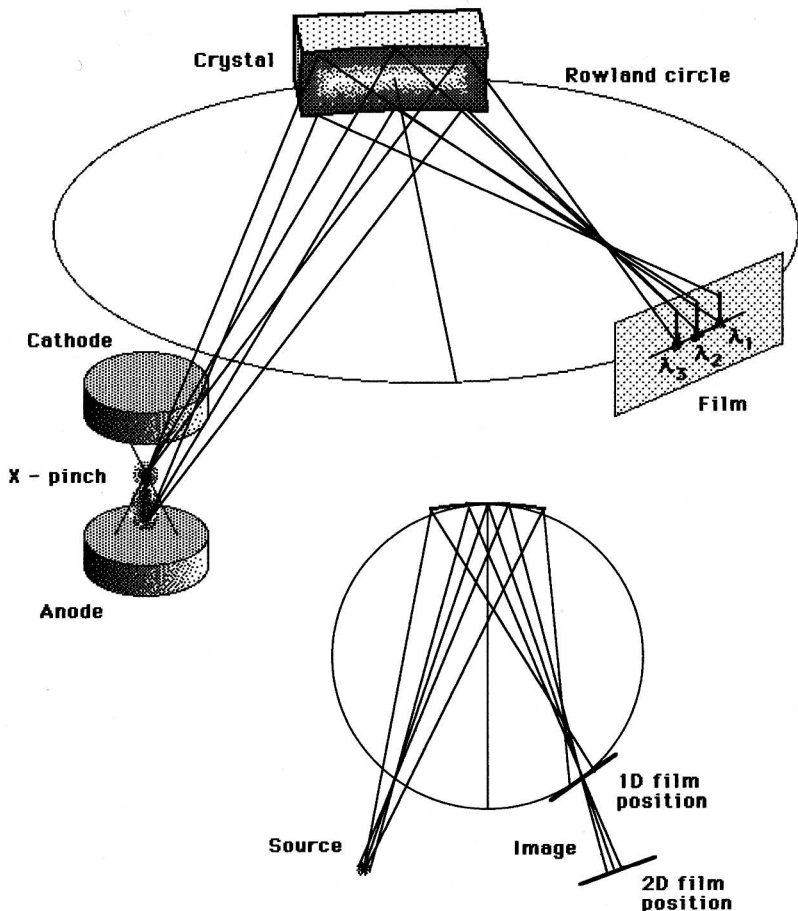


FIG. 2. Scheme of FSSR spectrograph.

for investigations of different plasma sources (4–7) and to obtain spectra with resolutions of up to $\lambda/\Delta\lambda = 10,000$ (7). It is necessary to point out that the aperture ratio in this geometry exceeds the aperture ratio of the Johann-type spectrograph by a factor of

$$G = (1 - 2a \sin \theta / (a + R \sin \theta))^{-1}. \quad [2]$$

This is due to the fact that vertical focusing approaches infinity in the case of total focusing on the saggital plane. In practice, however, G is limited by the aberrations of a spherical mirror and the quality of the crystal, and in our case G was between 100 and 500. As can be seen from [1], total focusing can only be achieved for the angles of incidence between 0 and 45°, which correspond to the wavelengths from

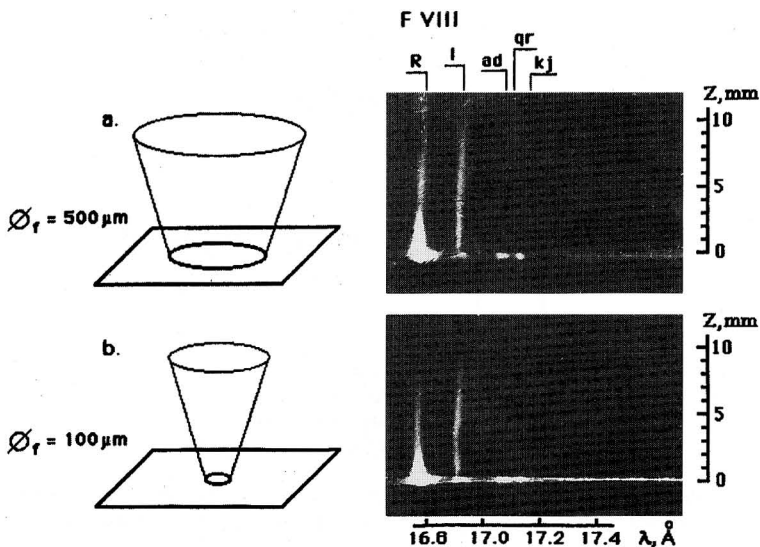


FIG. 3. Spectrograms of laser-produced plasma heated in different focus conditions with one-dimensional spatial resolution obtained by FSSR-1D spectrograph with $R = 100 \text{ mm}$ in first order of mica crystal reflection.

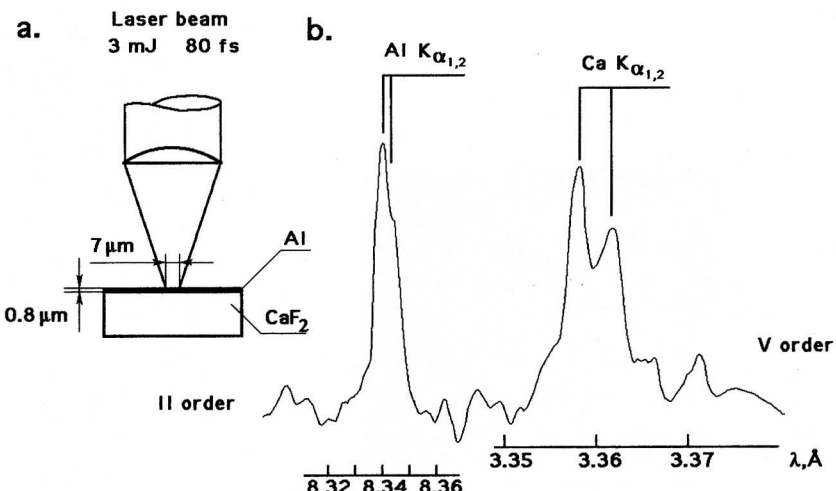


FIG. 4. Densitograms of K_{α} spectral lines of Al (II-order of reflection) and Ca (V-order of reflection), obtained in femtosecond laser-produced plasma by FSSR-1D spectrograph with $R = 100 \text{ mm}$ mica spherically bent crystal.

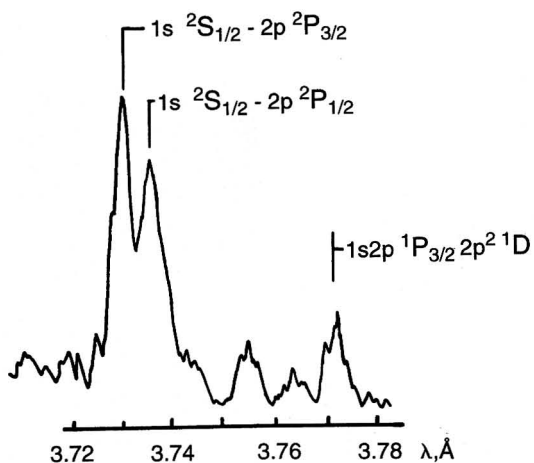


FIG. 5. Densitogram of H-like Ar spectrum from gas-puff Z-pinch (current 90 kA, pulse duration 1200 ns) obtained by FSSR-1D spectrograph with $R = 100$ mm mica spherically bent crystal in V order of reflection.

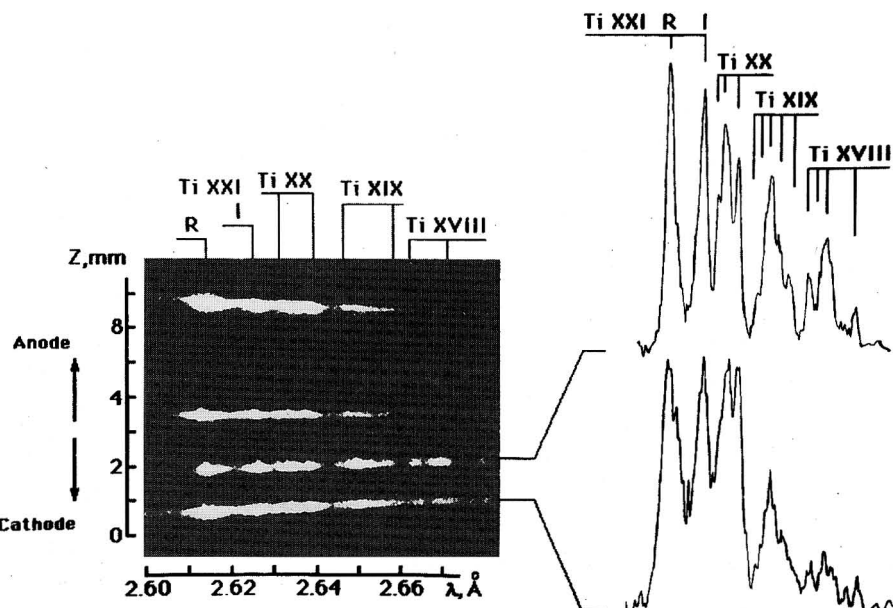


FIG. 6. Spectrograms and densitograms for various "hot spots" of Ti-wires Z-pinch plasma (current 250 kA, pulse duration 100 ns) in VII order of reflection. Satellite lines belonging to different isoelectronic sequences are marked.

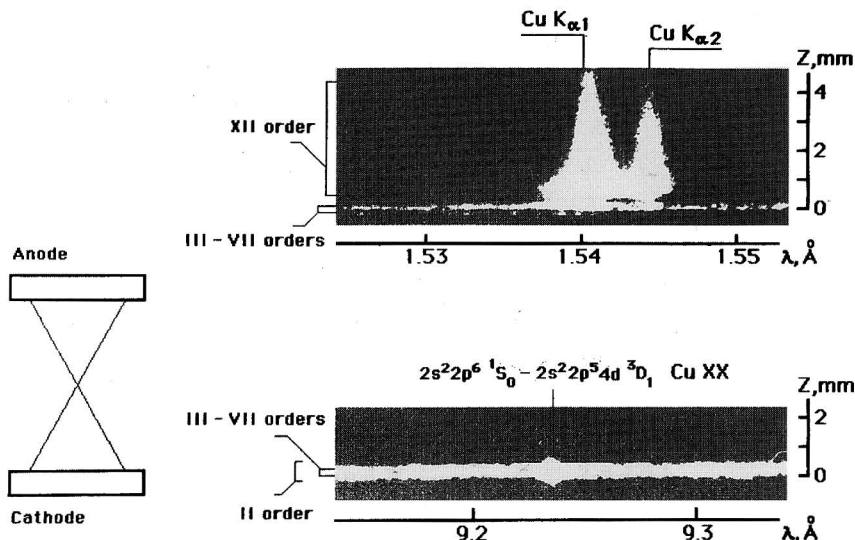


FIG. 7. Spectrograms of Cu-wires ($30 \mu\text{m}$) X-pinch (current 250 kA , pulse duration 100 ns) obtained by FSSR spectrograph with radius of crystal curvature $R = 250 \text{ mm}$ in II–XII-mica reflection orders. (a) Kodak DEF film, (b) Kodak RAR 2497 film.

$\sqrt{2}d/m$ to $2d/m$, where d is the crystal spacing and m is the order of reflection. This is why it is important for many applications that the employed crystals have high reflection orders. Mica crystal is unique in this case. It has very good reflectivity at I, II, III, IV, V, VII, VIII, XI, XII, and XIII orders of reflection (8). Several orders of reflection can be used to scan a very wide spectral range from 1.1 to $19,944 \text{ \AA}$ with a single mica spherical mirror.

The technology for manufacturing these high quality spherically curved mica crystals is thoroughly developed. A thin $30\text{-}\mu\text{m}$ mica crystal is glued onto a glass support, which has an optical surface with a curvature of radius equal to 100 , 186 , or 250 mm for use in our experiments. The details of the technology for preparing, cleaning, fixing, and gluing the mica crystals on the spherical surface are rather complicated and the process must be performed very carefully.

Illustrations of using spherical mica crystals in the FSSR-1D scheme are shown in Figs. 3–8. The pictures and densitograms of some spectra of multicharged ions from different plasma sources are presented. From these figures it is clear that one crystal can be used for measurements of the spectra in a wide spectral range from 1.1 to 17 \AA . Mica crystals have the very interesting property of having good reflections in many orders simultaneously, as illustrated in Figs. 4, 7, and 8. In Fig. 4 the densitograms of the K_{α} spectra of Al in II-order and the K_{α} spectra of Ca in V-order of reflection are presented (9). Both spectra were registered on the same film simultaneously and allow us to investigate the role of thickness of an Al cover in the case of femtosecond laser radiation interaction with a CaF_2 substrate. The fine structure of Cu-wire X-pinch plasma was investigated by using a $R = 250 \text{ mm}$ mica crystal spectrograph (Fig. 7).

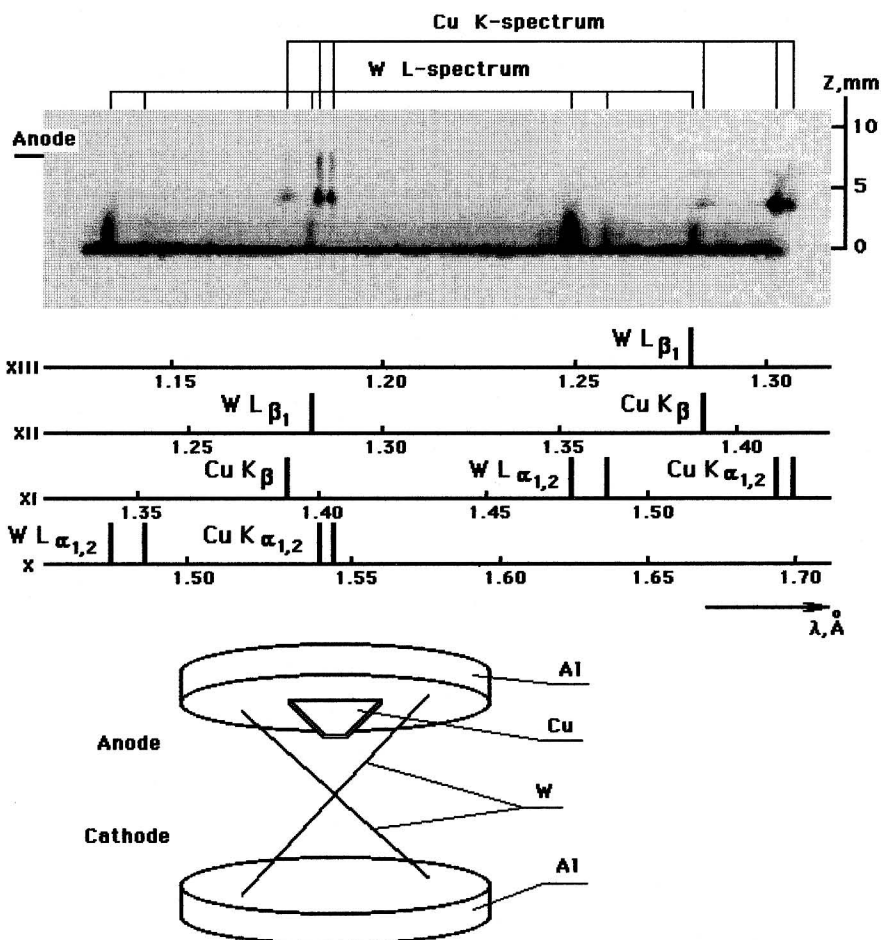


FIG. 8. Spectrum of W wires (25 μm) X-pinch (current 350 kA, pulse duration 100 ns) obtained by FSSR-spectrograph in X-XIII mica reflection orders. A piece of copper was placed on the anode for wavelength and scale calibration.

The high simultaneous reflectivity of mica crystals in the different orders permitted us to register the spectrum of Ne-like Cu (2nd order), K_α lines (12th order) with unique resolution and bremsstrahlung radiation from "hot spots" (3rd–7th orders). In this case, a two-film "sandwich" was used as the radiation recorder. The front film (Kodak RAR-2497) registered soft radiation, while the rear one (Kodak DEF) registered the hard components with $\lambda < 3 \text{ \AA}$. The capability for registration of the spectra in high-reflection orders (X–XIII) is nicely illustrated by Fig. 8.

As was discussed above, the FSSR-1D scheme enables us to obtain spectra with one-dimensional spatial resolution, which was limited by the laws of optics and the quality of the bent crystals. A spatial resolution of about 18 μm was experimentally

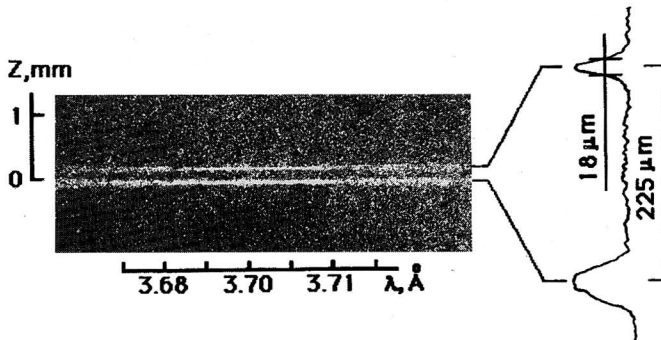


FIG. 9. Image of Pd wires X-pinch in the fifth order of mica crystal reflection obtained by FSSR spectrograph ($R = 100$ mm).

determined in Pd-wire X-pinch experiments (Fig. 9) for the spherically bent mica crystal with a 100 mm radius of curvature and dimension 10×30 mm.

Focusing spectrographs with two-dimensional spatial resolution (FSSR-2D). The dispersive properties of the crystals make it possible to obtain spatial resolution in the direction of dispersion (I). This possibility can be realized in the FSSR spectrograph too. In this case a radiation detector must be placed outside of the Rowland circle (see Fig. 2). The detailed investigation and application of the FSSR-2D scheme for plasma diagnostics were done in articles (1–3, 11). As was shown in publications (1, 11), the magnifications are equal in the sagittal plane to

$$S = b/a = R/(2a \sin \theta - R) \quad [3]$$

and in the meridional plane to

$$M = g/c = R[a - \sin \theta(2a \sin \theta - R)]/(R \sin \theta - a)(2a \sin \theta - R). \quad [4]$$

From Eqs. [3], [4] one can see that equal magnification in both planes can be obtained if $\theta = \pi/2$.

For many applications it is very useful to employ this FSSR-2D scheme in order to obtain images of rather large (approximately 1–15 mm) plasma sources in the radiation of separated spectral lines with wavelengths less than the crystal double spacing $2d$ ($\theta < \pi/2$). The variation of this FSSR-2D scheme with its source position outside of the Rowland circle enabled us to obtain two-dimensional images with some specific aberrations (see Fig. 10). The spatial resolution was still better than $100 \mu\text{m}$ in both directions even for distances from the target of about 15 mm. An example of a successful application of the mica spherical crystal with $R = 100$ mm for investigation of laser radiation interaction with targets of different shapes is presented in Fig. 11.

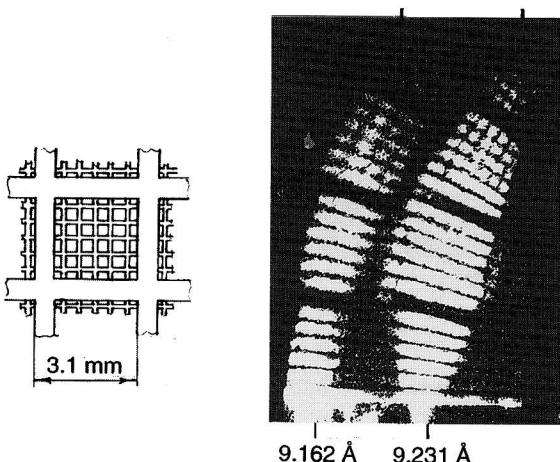


FIG. 10. Image obtained by FSSR-2D spectrograph with $R = 100$ mm mica crystal of two overlapping 100 μm and 500 μm wire meshes illuminated by laser produced plasmas.

The main characteristics of FSSR-1D- and FSSR-2D-type spectrographs are summarized in Table 1.

X-ray microscope. According to Eqs. [3] and [4], if $\theta = \pi/2$ or is close to $\pi/2$ the magnification can have any value. The use of normal angles is common in x-ray microscopes (*1*, *12*) and allows us to obtain monochromatic 2D images with spatial resolution of up to 5 μm . Figure 12 illustrates the usage of such an x-ray microscope

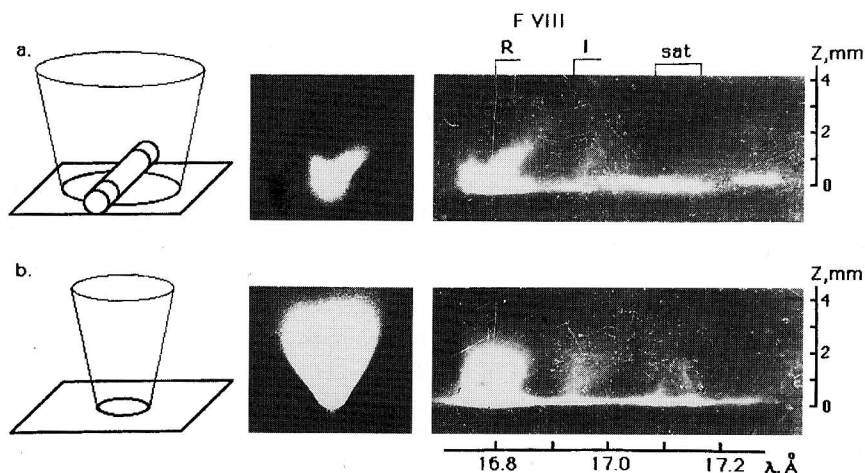


FIG. 11. The structure of radiation of target covered by Fe wire (diameter, 200 μm) (a) and flat CF_2 target (b) heated by Nd-glass laser (output energy 15 J, pulse duration 2 nsec). One can clearly see the correlation of images obtained by pinhole and FSSR-2D spectrograph with mica crystal ($R = 100$ mm).

TABLE 1

Parameters of FSSR 1D and 2D Spectrographs (Focusing Spectrograph with Spherically Bent Crystal and One- or Two-Dimensional Spatial Resolution)

Crystal	Mica	Quartz
Interplanar spacing $2d$, Å	19.9	8.512
Radius of curvature R , mm	100, 186, 250, 436	500
Crystal size, mm \times mm	10 \times 30, 15 \times 50	Diam. 30
Orders of reflection	I-V, VII, VIII, XI-XIII	I
Spectral range, Å	1.2-19	6.5-8.5
Spectral resolution, $\lambda/\Delta\lambda$	3,000-10,000	up to 20,000
Spatial resolution, μm	up to 15	up to 5

with a spherically bent ($R = 100$ mm) mica crystal for obtaining images of X-pinch when a very short wavelength emission is presented (10).

Forming of X-ray parallel beams. Another interesting application of this crystal could be achieved by placing a plasma source in a crystal mirror focus. In a manner it is possible to create intensive monochromatic collimated beams of soft x-rays in the 4-10 Å spectral range with a divergence angle of about 5×10^{-4} rad (13-15). In Fig. 13 a photo of a beam at a distance of 40 cm from the spherical mica crystal with $R = 100$ mm is presented (16). The shadowgram of two overlapping wire meshes

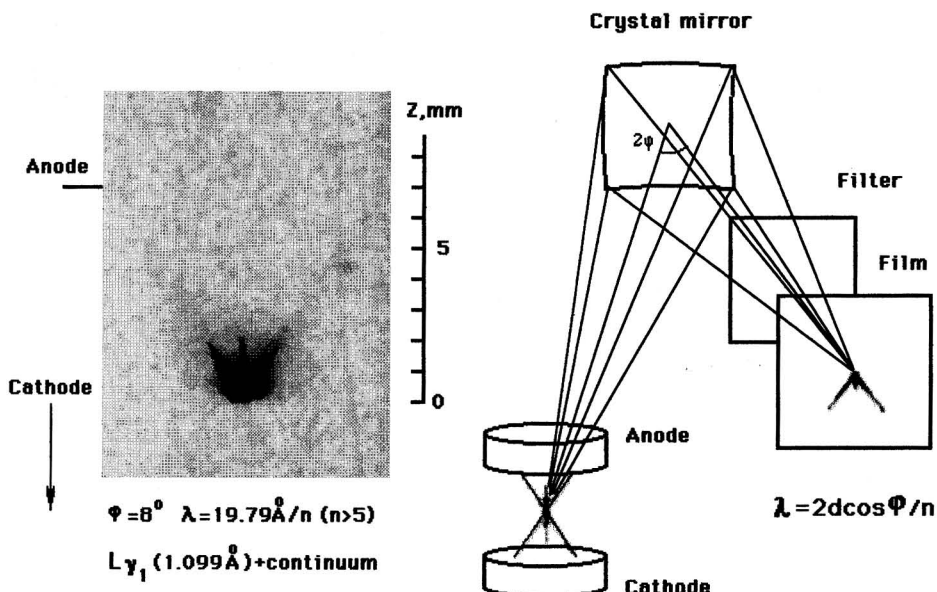


FIG. 12. X-ray microscope image of W wire X-pinch. Mica crystal, $R = 186$ mm.

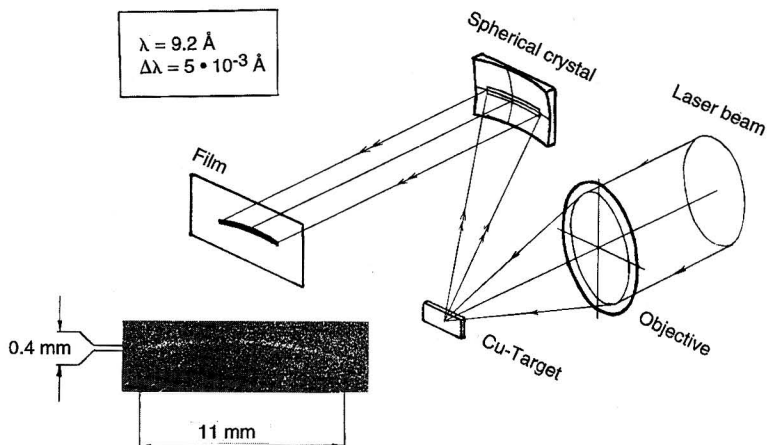


FIG. 13. The scheme of experiments for obtaining parallel monochromatic beams using spherically bent mica crystal with $R = 100$ mm. Film-to-crystal distance is 40 cm; second order of mica crystal reflection was used.

is shown in Fig. 14. The x-ray parallel beam of X-pinch radiation was produced by the 100-mm radius crystal (15).

Monochromatic backlighting. Spherically bent crystals can also be successfully used for obtaining x-ray absorption images of different plasma sources (backlighting). A schematic of such an experiment is presented in Fig. 15. Here the source of x-ray radiation is placed on the Rowland circle, and a large crystal aperture is used for the single wavelength. Positions of the investigated object and the radiation receiver are determined by the lens formula $1/f = 1/a + 1/b$, where f is the focal length of the spherically bent crystal and the spatial resolution is determined by spherical aberrations

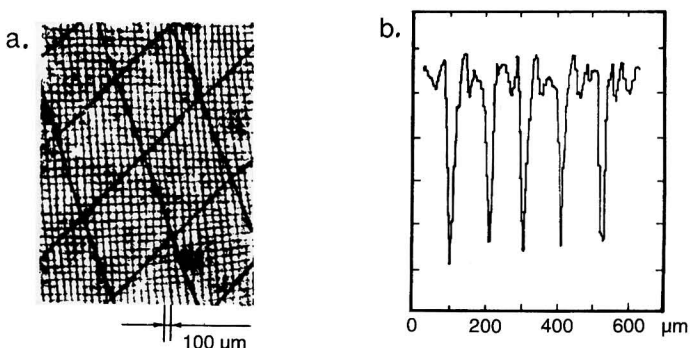


FIG. 14. Shadowgram and densitogram of two overlapping wire meshes obtained in parallel beam of X-pinch (current 250 kA, pulse duration 100 ns, load 0.03 mm diameter Cu wires) radiation formed by spherically bent mica crystal with $R = 100$ mm in second order of reflection.

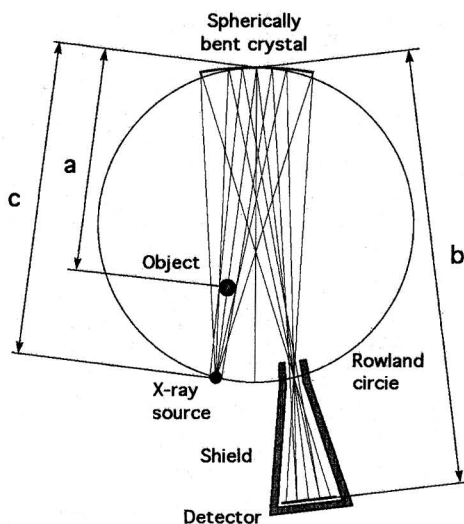
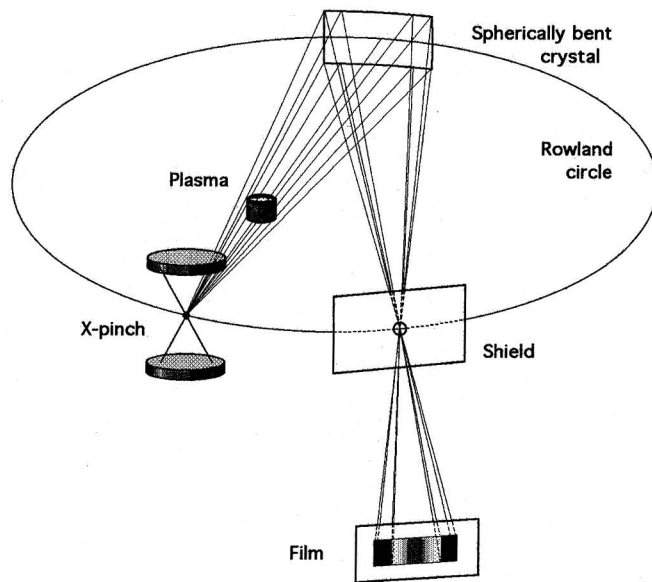
a.**b.**

FIG. 15. Principal scheme of monochromatic x-ray backlighting (a) and its possible realization with X-pinch source (b).

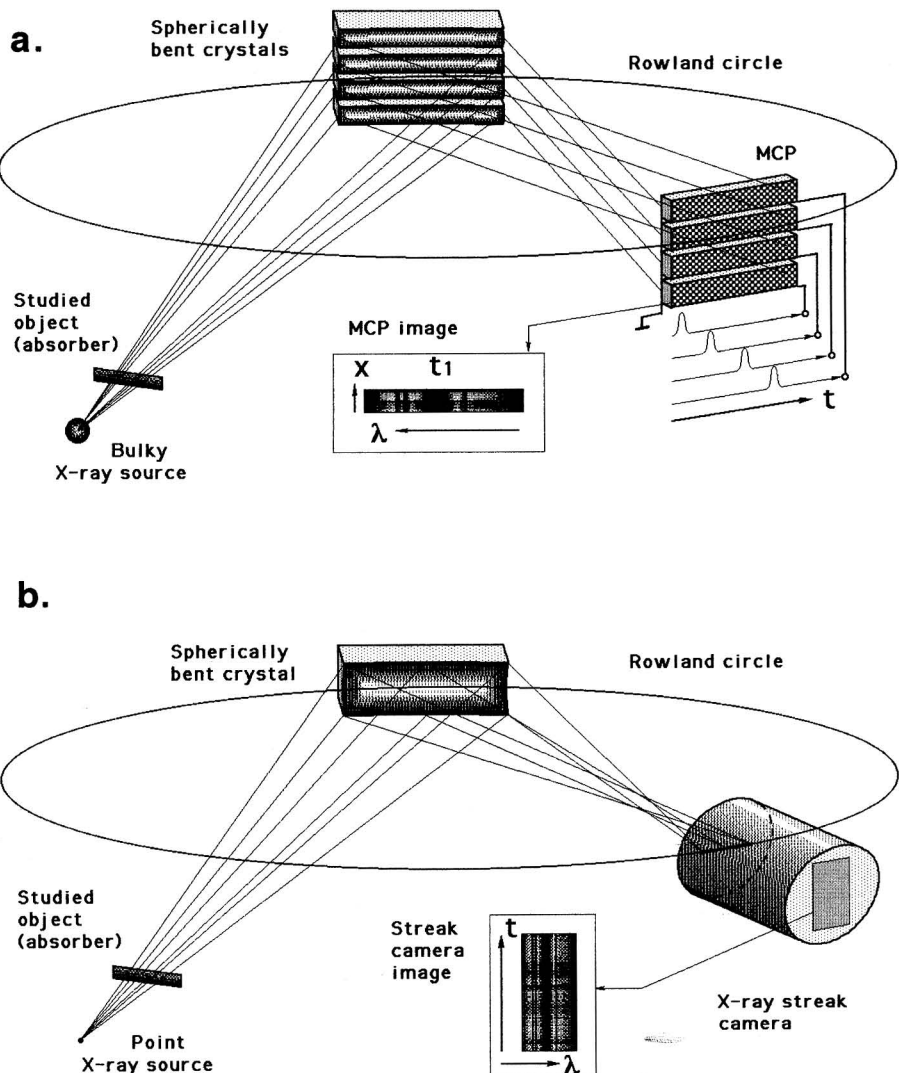


FIG. 16. Schemes for using the spherically bent crystals for x-ray absorption spectroscopy: (a) obtaining of frame absorption spectra with one-dimensional spatial resolution, (b) obtaining time-resolved absorption spectra.

and is independent of the source size. Moreover, the possibility of using a very dense shield with a pin-hole entrance to protect the receiver from self radiation from the investigated plasma objects is also important here.

X-ray absorption spectroscopy. Absorption spectroscopy requires very high luminosity of the x-ray optical elements, and spherically bent crystals may be utilized for

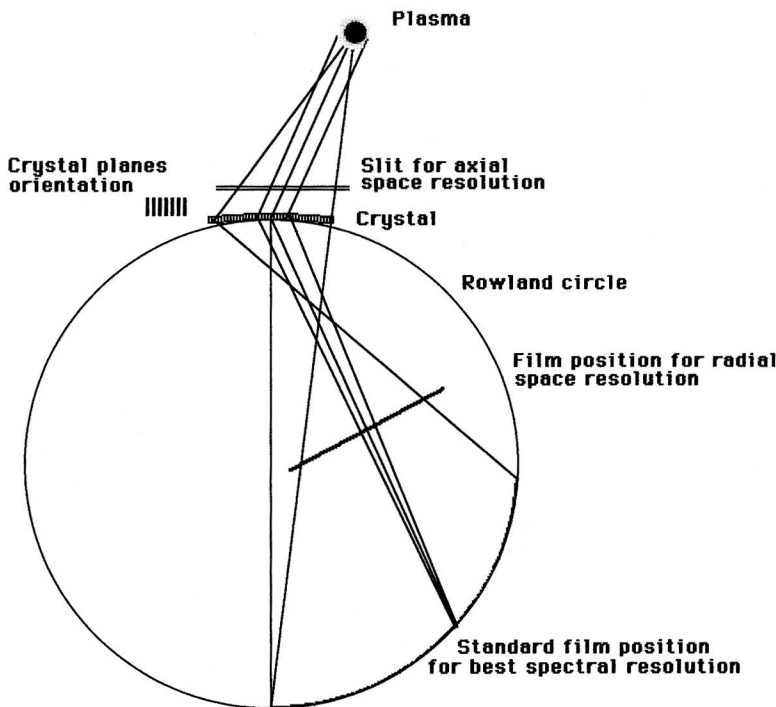


FIG. 17. Cauchois imaging spectrograph scheme.

designing very effective devices for this purpose. Figure 16 shows two proposals for absorption experiments. The first one (Fig. 16a) includes a four-crystal analyzer and a four-microchannel plate (MCP) receiver for registering the absorption spectra with one-dimensional spatial resolution at different time intervals. In this case the source of radiation must be of a size comparable to the size of the object investigated. The object images are focused on the MCP surfaces. The second scheme (Fig. 16b) is based on a single-crystal analyzer and x-ray streak camera. In this scheme it is more convenient to use the point x-ray source (an X-pinch, for example) in order to eliminate the positioning of the entrance slit in front of the photocathode. The image of the source is focused on the photocathode surface to increase the luminosity of the system.

CAUCHOIS IMAGING SPECTROGRAPH

Certain difficulties arise in the short wavelength region of the spectrum ($\lambda \sim 1-3$ Å) upon using "reflection" spectrographs (for example, Johann or even FSSR types). These difficulties are connected with the fact that not many crystals have reasonable reflectivity in this spectral range. In this case the Cauchois-type spectrograph (see Fig. 17) is most appropriate for investigation of the short-wavelength radiation. It is possible to place a slit parallel to the spectral dispersion of the crystal to obtain spectra with one-dimensional spatial resolution. This is analogous to the flat or Johann-type

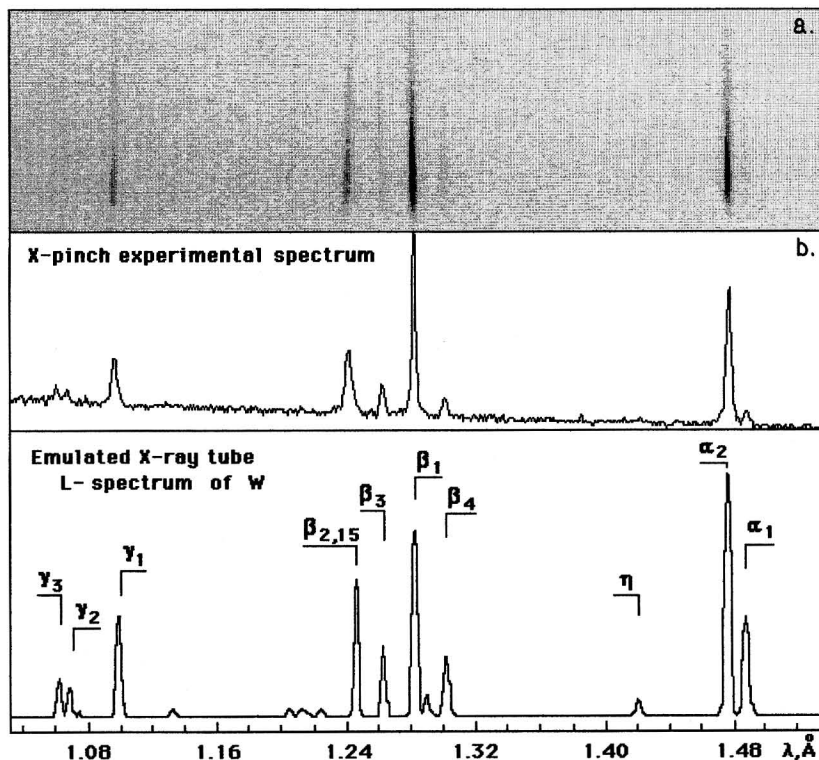


FIG. 18. W wires ($25 \mu\text{m}$) X-pinch (current 350 kA , pulse duration 100 ns) spectrum (a) and its densitogram (b) obtained by a Cauchois spectrograph with standard film position and spectrum of x-ray tube.

spectrograph. In Fig. 18 a densitogram of the spatially resolved spectra emitted by an X-pinch plasma in the spectral range 1.02 – 1.49 \AA is presented (10). It is obvious that a Cauchois-type spectrometer produces intensive spectra with good spectral and spatial resolution.

Some new applications of the Couchois scheme can be obtained by placing the film outside of the Rowland circle (see Fig. 17), analogous to the FSSR-2D scheme (10). In Fig. 19 one can see the possibility of obtaining very good two-dimensional monochromatic images of very short wavelength radiation. The two-dimensional pictures show bright radiation from the wire cores and a jet on the anode side of the pinch. The spectra in this range consist of lines corresponding to transitions in neutral or just a few times ionized W. In these experiments (10) the Cauchois-type spectrometer was also successfully used to register x-ray radiation with wavelengths near 0.49 \AA (K_β line of silver).

CONCLUSIONS

By using the above described devices, one can investigate the x-ray radiation of plasma microsources in the wide spectral range 1 – 20 \AA with high spatial (10–20

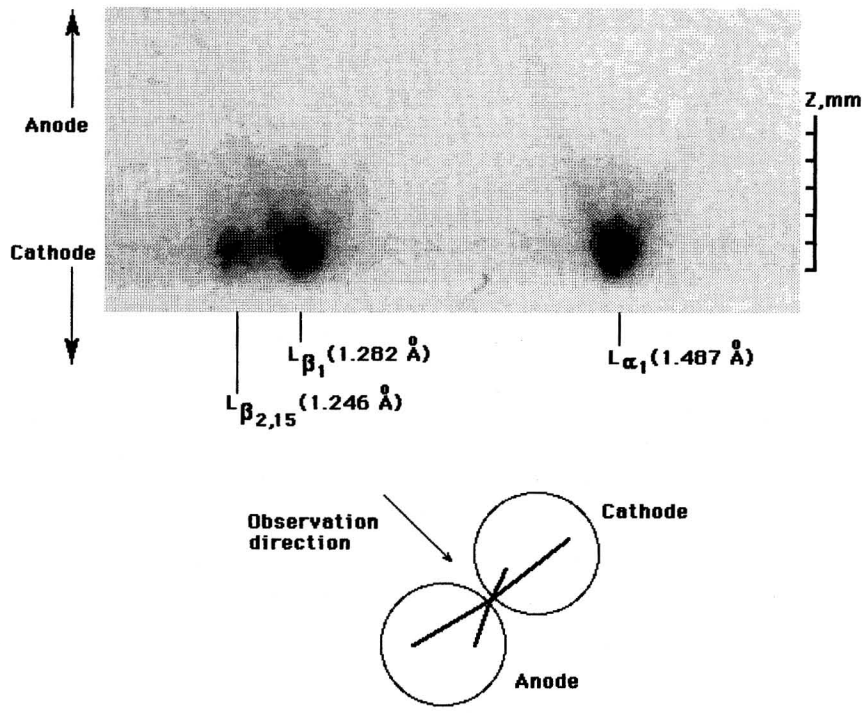


FIG. 19. Two-dimensional images of W wires ($25 \mu\text{m}$) X-pinch in radiation of separate spectral lines obtained with imaging Cauchois spectrograph.

μm) and spectral ($\Delta\lambda/\lambda \sim 3,000\text{--}10,000$) resolution. It is also possible to obtain high-quality monochromatic images of plasma sources for this entire spectral range.

ACKNOWLEDGMENTS

This work was partially supported by Russian Fundamental Science Foundation Grant 93-02-15410 and by International Science Foundation Grant MJB000.

REFERENCES

1. V. A. BOIKO, A. V. VINOGRADOV, S. A. PIKUZ, I. YU. SKOBELEV, AND A. YA. FAENOV, *J. Sov. Laser Res.* **6**, 85 (1985).
2. B. A. BRYUNETKIN, S. A. PIKUZ, I. YU. SKOBELEV, AND A. YA. FAENOV, "Laser and Particle Beams," Vol. 10, p. 849, 1992.
3. A. YA. FAENOV, S. A. PIKUZ, A. I. ERKO, B. A. BRYUNETKIN, V. M. DYAKIN, G. V. IVANENKOV, A. R. MINGALEEV, T. A. PIKUZ, V. M. ROMANOVA, AND T. A. SHELKOVENKO, *Physica Scripta* **50**, 333 (1994).
4. S. A. PIKUZ, B. A. BRYUNETKIN, G. V. IVANENKOV, A. R. MINGALEEV, V. M. ROMANOVA, I. YU. SKOBELEV, A. YA. FAENOV, S. YA. KHAKHALIN, AND T. A. SHELKOVENKO, *JQSRT* **51**, 291 (1994).
5. S. YA. KHAKHALIN, V. A. DYAKIN, A. YA. FAENOV, C. YA. KHAKHALIN, V. M. DYAKIN, A. YA.

- FAENOV, H. FIEDOROWICZ, A. BARTNIK, P. PARYS, J. NILSEN, AND A. OSTERHELD, *Physica Scripta* **51**, 352 (1995).
6. J. NILSEN, P. BEIRSDORFER, S. R. ELLIOTT, T. W. PHILLIPS, B. A. BRYUNETKIN, V. M. DYAKIN, T. A. PIKUZ, A. YA. FAENOV, S. A. PIKUZ, S. VON GOELER, M. BITTER, P. A. LOBODA, V. A. LYKOV, AND V. YU. POLITOV, *Phys. Rev. A* **50**(3), 2143 (1994).
 7. B. A. BRYUNETKIN, I. YU. SKOBELEV, A. YA. FAENOV, M. P. KALASHNIKOV, P. NICKLES, M. SHNURER, AND S. A. PIKUZ, *Quantum Electronics* **23**(4), 337 (1993).
 8. S. A. PIKUZ, V. M. ROMANOVA, T. A. SHELKOVENKO, T. A. PIKUZ, A. YA. FAENOV, E. FORSTER, J. WOLF, AND O. WEHRHAM, *Quantum Electronics* **25**(1), 16 (1995).
 9. J. P. GEINDRE, P. AUDEBERT, A. ROUSSE, J. C. GAUTHIER, A. YA. FAENOV, T. A. PIKUZ, S. A. PIKUZ, AND T. A. SHELKOVENKO, *J. X-Ray Sci. Technol.*
 10. S. A. PIKUZ, V. M. ROMANOVA, T. A. SHELKOVENKO, D. A. HAMMER, AND A. YA. FAENOV, Spectroscopic investigations of the x-ray spectra from X-pinch plasmas, in "Proceedings of the Beam-94 Conference, June 20-24, 1994, San Diego," Vol. 2, p. 764.
 11. B. A. BRYUNETKIN, V. M. DYAKIN, S. A. PIKUZ, T. A. PIKUZ, AND A. YA. FAENOV, *Quantum Electronics* **24**(2), 356 (1994).
 12. E. FORSTER, K. GABEL, AND I. USCHMANN, *Laser and Particle Beams* **9**, 135 (1991).
 13. A. YA. FAENOV, Y. A. AGAFONOV, B. A. BRYUNETKIN, A. I. ERKO, G. V. IVANENKOV, A. R. MINGALEEV, V. M. ROMANOVA, I. YU. SKOBELEV, AND T. A. SHELKOVENKO, "Proceedings of SPIE-93 Annual Meeting, Applications of Laser Plasma Radiation, July 14-16, 1993, San Diego," Vol. 2015, p. 63.
 14. M. SCHNURER, P. V. NICKLES, M. P. KALASHNIKOV, F. BILLHARDT, A. YA. FAENOV, AND B. A. BRYUNETKIN, "Proceedings of SPIE-93 Annual Meeting, Applications of Laser Plasma Radiation, July 14-16, 1993, San Diego," Vol. 2015, p. 260, 1993.
 15. A. YA. FAENOV, A. R. MINGALEEV, S. A. PIKUZ, T. A. PIKUZ, V. M. ROMANOVA, I. YU. SKOBELEV, AND T. A. SHELKOVENKO, *Quantum Electronics* **23**(5), 394 (1993).
 16. S. BOLLANTI, P. Di LAZZARO, F. FLORA, G. GIORDANO, T. LETARDI, G. SCHINA, C. E. ZHENG, L. FILIPPI, L. PALLADINO, A. REALE, G. TAGLIERI, D. BATANI, A. MAURI, M. BELLI, A. SCAFATI, L. REALE, P. ALBERTANO, A. GRILLI, A. FAENOV, T. PIKUZ, AND R. COTTON, *J. X-Ray Sci. Technol.* **5**(3), 261 (1995).